The quantum Zeno effect: a solvable model for indirect pre-measurements

2004 J. Phys. A: Math. Gen. 37 11285

(http://iopscience.iop.org/0305-4470/37/46/013)

INSTITUTE OF PHYSICS PUBLISHING JOURNAL OF PHYSICS A: MATHEMATICAL AND GENERAL

J. Phys. A: Math. Gen. **37** (2004) 11285–11308 PII: S0305-4470(04)82100-0

The quantum Zeno effect: a solvable model for indirect pre-measurements

Anil Shaji

The University of Texas at Austin, Center for Statistical Mechanics, 1 University Station C1609, Austin TX 78712, USA

E-mail: shaji@physics.utexas.edu

Received 11 June 2004, in final form 27 September 2004
Published 3 November 2004
Online at stacks.iop.org/JPhysA/37/11285
doi:10.1088/0305-4470/37/46/013

Abstract

A simple model of indirect pre-measurements on an unstable quantum state is presented in this paper. The model is completely solvable and the solutions are used to compare the time evolution of the unstable state with and without the influence of the pre-measurement. We find that by choosing the details of the process of pre-measurement appropriately, it is possible to observe both suppression and enhancement of the rate of decay of the unstable state. When the pre-measurements are assumed to lead on to actual measurements, we see that the quantum Zeno effect, and in some instances the 'anti-Zeno' effect, can be produced by repeating the measurement many times in succession. The Zeno effect can appear in our model either as a real consequence of repeated measurements or sometimes merely as an artefact of the manner in which the observations on the system are performed. The anti-Zeno effect appears almost exclusively as an artefact of the details of the measurement. Numerical investigations are included to delineate the regimes in which the quantum Zeno effect and possibly the anti-Zeno effect can occur.

PACS numbers: 03.65.Ta, 03.65.Xp

1. Repeated measurements and the quantum Zeno effect

The quantum Zeno effect [1] is so closely connected to quantum measurements that a complete understanding of one is not possible without the other. Quantum measurement theory still being a work in progress [2–5], this paper is an effort to use what we do know of the act of measuring a quantum system to gain further insights into the Zeno effect. We construct a model of indirect pre-measurements on an unstable quantum state which is closely related to the Cascade model of interacting quantum systems [6] and use it to investigate the appearance of the Zeno effect when the state is subjected to repeated observations. Within the context of

the model we look at the possibility that non-ideal measurements can lead to the anti-Zeno or inverse-Zeno effect [7–10]. We also discuss the question whether exploration of the quantum Zeno and anti-Zeno effects can provide clues to a better understanding of the nature of quantum measurements.

Continuous observation of a quantum system can, in principle, arrest its time evolution entirely. This is the quantum Zeno effect [1]. The existence of an operator $T(t)$ corresponding to continuous measurement and belonging to the Hilbert space of the observed system was shown in [1] where,

$$T(t) \equiv \lim_{N\to\infty} (\mathrm{e}^{\mathrm{i}Ht/N} E\, \mathrm{e}^{-\mathrm{i}Ht/N})^N. \tag{1}$$

E is a projective measurement of the von Neumann type [11] interspersed with Hamiltonian evolution. The convergence of the limit in the definition of $T(t)$ and the experimental realizability of ideal projective measurements are two issues regarding the Zeno effect that have been discussed extensively in the literature [12–15]. Several proposals can be found [16, 17] for replacing the idealized operator $T(t)$ with a more 'realistic' one.

Treating measurements on a quantum system in a more detailed fashion than just as a projection led to the identification of the possibility that the act of measurement can not only suppress but in some cases apparently speed up the evolution. This is the quantum anti-Zeno effect. Several mechanisms have been suggested that can lead to the anti-Zeno effect [7–10] to the point that Kofman and Kurizki [9] conclude that the anti-Zeno effect is a more natural and easily observable one in a generic quantum system which is subjected to 'realistic' measurements. A realistic measurement being one that occurs in a finite amount of time and admits the possibility of being viewed as a process [18] rather than being an instantaneous, discontinuous event such as the von Neumann projection. The problem, though, is that analytic and numerical investigations of various scenarios involving realistic measurements lead to at best different—but more often opposing—conclusions about the presence or absence of the quantum Zeno and anti-Zeno effects in measured systems [19–21].

Experiments by Itano *et al* [22] and more recently by Wunderlich *et al* [23] and Fischer *et al* [24] have successfully demonstrated the existence of the quantum Zeno (and anti-Zeno) effect in atomic systems, giving experimental support to the status of $T(t)$ as an observable. Earlier, Valanju had shown indirect evidence for the Zeno effect in hadron–nucleus collisions in which several interactions occur in rapid succession [25]. The experimental support for the anti-Zeno effect in [24] depends quite strongly on the details of the system that is being measured and the precise nature of its time evolution in the *absence* of the measurements. This makes it difficult to determine the role of the measurements in producing the anti-Zeno effect. The appearance of the anti-Zeno effect in the experiment described in [24] will be investigated in detail in a separate paper [26].

The common theme in the measurements, ideal or not, is that the quantum system that is observed is disturbed in some way or the other by the measurement. The measuring device is a physical system that must be sensitive to the microscopic dynamics of the quantum system it is observing while at the same time displaying the result of the measurement as a robust classical signal. To incorporate these two requirements it is convenient to view the measuring apparatus as being made up of two distinct parts. One part with a purely quantum character that couples directly with the system being observed and another part that transforms the signal from this coupling into a classical one. The motivation for splitting the measurement in this manner is to see if the disturbance on the observed quantum system can be treated in a deterministic fashion while treating the rest of the measurement in a probabilistic way.

A *spectral resolution* [27] of the quantum system being observed is achieved by the initial coupling of some part of the detector to it. Following Peres [28] we call the process that

achieves the spectral resolution a *pre-measurement*. This is a purely dynamical process governed by a Hamiltonian. The initial state of the system and the apparatus may be assumed to be a separable one: $|\Psi_0\rangle_{\rm SA} = \sum_n \alpha_n |a_n\rangle_S \otimes |A_0\rangle_A$ where $|a\rangle_S$ denote states of the system, $|A\rangle_A$ denote states of the apparatus and $\sum_n |\alpha_n|^2 = 1$. The net result of the pre-measurement is to entangle the system to the apparatus leading to a combined state of the form $|\Psi_t\rangle_{\rm SA} = \sum_n \alpha_n |a_n\rangle_S \otimes |A_n\rangle_A$. Extracting a macroscopic signal that is correlated to the state of the observed system from the entangled state $|\Psi_t\rangle_{\rm SA}$ completes the measurement. This would be equivalent to picking out only one of the terms in the expression for $|\Psi_t\rangle_{\rm SA}$ with probability $|\alpha_n|^2$. The last step is a non-unitary operation since it transforms a pure state of the system and the apparatus into a mixed state. Gaps remain in our understanding of how it can be achieved. For a discussion of the issues and subtleties involved, including the 'collapse' of the wavefunction and mechanisms like decoherence for achieving the collapse, we refer the reader to [3] and references therein.

This paper deals primarily with the relationship between quantum Zeno (and anti-Zeno) effect and pre-measurement. What happens when pre-measurements lead to complete measurements that produce classically observable signals is not discussed in detail. This is because at some point the consequences of the non-unitary, second part of the act of measuring a quantum system has to be inserted in an *ad hoc* fashion without specifying the dynamics (if any) that is involved. The complete measurements themselves have to be repeated with a high enough frequency in order to observe the quantum Zeno effect. Complete measurements and their repetitions that modify the evolution of the measured system are discussed only briefly in what follows. The focus is on how the pre-measurements can lead to conditions suitable for observation of the quantum Zeno and possibly anti-Zeno effects *provided complete measurements are performed and repeated at appropriate frequencies*.

We restrict our attention to quantum dynamics involving decay processes through the rest of this paper. The Zeno effect has been investigated previously by several authors in the context of the dynamics of unstable quantum systems [29–34]. The Hilbert space of the quantum systems we consider contains one or more unstable states which can decay into some other states within the same space. The prototypical model of a decaying unstable quantum state $|\Psi\rangle$ is characterized by an exponential decrease of its survival probability:

$$|\langle\Psi|\,\mathrm{e}^{-\mathrm{i}Ht}|\Psi\rangle|^2 = P(t) \simeq \mathrm{e}^{-\gamma_0 t} \tag{2}$$

where γ_0 is the (constant) decay rate [35]. Considerations based on model independent assumptions such as the positivity of energy, time reversal invariance ($P(t) = P(-t)$) and analyticity of the survival probability show that the purely exponential decay cannot hold strictly at all times [36–38]. Both short and long time behaviour of the survival probability of a generic unstable state must show deviations from the exponential decay law. The short time behaviour, which is usually quadratic in time, is of interest to us in the context of the quantum Zeno effect [39]. Sometimes the term 'Zeno effect' has been used to refer primarily to the deviation of $P(t)$ from purely exponential decay at short times. We note here that the quadratic dependence of the survival probability that is crucial for obtaining the Zeno effect is still only half the story. The other half lies in exploiting the slow initial decay by some means to arrest the evolution of the system. Slow, non-exponential behaviour of the survival probability at short times merely indicates the potential for observing the Zeno effect in the system. Repeated measurements or other interactions that 'resets' the system periodically so that it is never allowed to leave the non-exponential regime is what makes things interesting and manifests itself as the Zeno effect.

It is useful to approximate the behaviour of $P(t)$ including the modifications at short and long times with

$$P(t) \simeq \mathrm{e}^{-\gamma(t)t}, \tag{3}$$

where the effective decay constant $\gamma(t)$ acquires a time dependence [10]. $\gamma(t)$ is equal to the decay constant γ_0 in equation (2) except at short and very long times. In terms of the effective decay constant $\gamma(t)$ the time dependence of the survival probability of a decaying quantum state subject to frequent measurements τ seconds apart can be expressed as

$$P(t) = [P(\tau)]^N \simeq \mathrm{e}^{-\gamma(\tau)N\tau} \simeq \mathrm{e}^{-\gamma(\tau)t} \tag{4}$$

where $t = N\tau$ is taken to be the duration of the experiment, assuming that the measurements themselves takes only a negligible amount of time.

The repeated observations modify the effective decay constant γ_0 of the freely evolving state to a new constant value $\gamma(\tau)$. If τ is such that $\gamma(\tau) < \gamma_0$, we may call the resulting evolution the quantum Zeno effect. If we can find a τ such that $\gamma(\tau) > \gamma_0$ we have the possibility of obtaining the anti-Zeno effect. If there exists a τ^* such that $\gamma(\tau^*) = \gamma_0$ then by measuring the system at intervals of τ^* we can observe its natural decay as if no measurements were performed on it. In most cases it is easy to identify an interruption time τ that leads to the Zeno effect even though its value may be too small to be within the time resolution of a given experiment. The condition $\gamma(\tau) > \gamma_0$ required to observe the anti-Zeno effect need not always be satisfied for any τ as pointed out by Facchi, Nakazato and Pascazio in [10].

Following the lines of Koshino and Shimizu [40, 41] we try to make some inroads into the problem of understanding the Zeno and anti-Zeno effects in decaying systems by considering a process which may roughly be described as (a sequence of) '*indirect pre-measurements*' on the unstable quantum state. An indirect measurement being one in which the decay products of an unstable state are detected rather than observing the decaying unstable state directly. The model of indirect pre-measurements we present is similar to the model of 'continuous measurements' used by Schulman [42] to study the Zeno effect. Our focus is on how the pre-measurements affect the critical repetition rate τ of complete measurements that may lead to either the Zeno or anti-Zeno effects.

The organization of this paper is as follows: section 2 introduces the model of indirect pre-measurements and its solutions that are relevant in the current context. Section 3 considers the evolution of the system when the pre-measurements are not present for comparison with the case where the pre-measurements are present. The evolution of the system with the pre-measurements is discussed in detail in section 4. In section 5 we see how repeated measurements on the system can lead to Zeno effects and sometimes anti-Zeno effects. Concluding remarks are given in section 6.

2. Modelling indirect pre-measurements

The model we are considering is a completely solvable field theory of five interacting fields labelled by A, B, C, Θ and Φ. The basic commutation relations between the field operators are

$$[a, a^\dagger] = [b, b^\dagger] = [c, c^\dagger] = 1$$
$$[\theta(\omega), \theta^\dagger(\omega')] = \delta(\omega - \omega'); \qquad [\varphi(\nu), \varphi^\dagger(\nu')] = \delta(\nu - \nu')$$

with lowercase letters a, b, c, θ, φ $(a^\dagger, b^\dagger, c^\dagger, \theta^\dagger, \varphi^\dagger)$ denoting the annihilation (creation) operators of the corresponding fields. All other commutators are identically zero. The fields Θ and Φ are labelled by continuous parameters $0 \leqslant \omega, \nu \leqslant \infty$ while the A, B and C

are characterized by discrete labels. The number of interacting fields and their commutation relations are identical to the Cascade model worked out in [6]. The model we are considering here differs from the Cascade model only in the details of the interactions between the fields and thereby in the processes that are allowed in the theory.

We want to construct a dynamical system using these five fields that represents both the decay of an unstable quantum state and a (quantum) process that may be viewed as a measurement, or at least a precursor to a measurement, being performed on the unstable state.

2.1. Indirect pre-measurements

The determination of whether an unstable state has decayed or not can be done in two ways. Measurements may be made on the state itself to determine if it is remaining intact. This would correspond to a direct measurement of the survival probability. The indirect method is to introduce a detector that is sensitive only to the decay products which are produced when the original state disintegrates. The model that we are considering is of the latter kind where we assume that the original unstable state $|A\rangle = a^\dagger|0\rangle$ is never directly observed but the presence of the decay product $|B\Theta\rangle = b^\dagger\theta^\dagger(\omega)|0\rangle$ is detected by coupling it with an excitation $|C\Phi\rangle = c^\dagger\varphi^\dagger(\nu)|0\rangle$ that is assumed to be induced in (some part of) the detector. In other words, this method is known as '*indirect pre-measurement*' (also called *continuous measurement* in [42]).

A useful analogy to visualize the processes that are happening in the model is to consider the states $|A\rangle$ and $|B\rangle$ as the excited and ground states of an atom respectively. $|\Theta\rangle$ can then be thought of as a photon that is emitted when the excited state decays into the ground state. The photon, in turn, is detected by a photodetector which emits an elementary excitation $|\Phi\rangle$, an electron for instance, causing the state of (some part of) the detector to become $|C\rangle$. Like all analogies, this one should also be used with caution because our model is too simple to accurately model all the details of a real atomic system unless a lot of restrictions are placed on the real system.

The creation of the mode $|\Phi\rangle$ does not constitute an 'observation' unless the excitation is amplified to produce a classical signal such as the current in a photo-multiplier tube. The problem in going through with the production of such a macroscopic signal in our treatment is that it would imply the destruction of the state $|\Phi\rangle$. In the context of understanding the quantum Zeno and anti-Zeno effects, what is of interest to us is to see how the presence of the $|\Phi\rangle$ state in the system affects the evolution of the original unstable state $|A\rangle$. If we go through with the whole measurement and assume that the excitation in the detector has been destroyed as part of the detection process then this state cannot possibly affect the time evolution of $|A\rangle$ any longer. If we assume that any realistic measurement takes a finite interval of time to perform then we expect that excitations in the Φ and A fields can exist simultaneously and interact during that finite interval. This is the reason why, as a first step, we consider only the effect of a pre-measurement consisting of the production of $|\Phi\rangle$ on the evolution of $|A\rangle$.

2.2. Allowed processes and the Hamiltonian

The processes that are present in our model of indirect pre-measurements are

$$A \rightleftharpoons B\Theta; \qquad B\Theta(\omega) \rightleftharpoons BC\Phi(\nu). \tag{5}$$

We note here that field theoretic models constructed along similar lines were considered by Panov [43] and by Facchi and Pascazio [44] to study the quantum Zeno effect. The models in [43, 44] differ significantly from the present one in the number of fields involved and the interactions that are allowed.

The Hamiltonian of the model is

$$H = H_0 + V, \tag{6}$$

$$H_0 = m_A A^\dagger A + m_B B^\dagger B + \int_0^\infty \mathrm{d}\omega\, \omega \theta^\dagger(\omega)\theta(\omega) + \int_0^\infty \mathrm{d}\nu\, \nu \varphi^\dagger(\nu)\varphi(\nu), \tag{7}$$

$$V = \int_0^\infty \mathrm{d}\omega [f^*(\omega) A^\dagger B \theta(\omega) + f(\omega) B^\dagger \theta^\dagger(\omega) A] + \int_0^\infty \mathrm{d}\omega \int_0^\infty \mathrm{d}\nu [G^*(\omega, \nu)\theta^\dagger(\omega) C \varphi(\nu) + G(\omega, \nu) C^\dagger \varphi^\dagger(\nu)\theta(\omega)]. \tag{8}$$

In writing the Hamiltonian, the rotating wave approximation has been used and the mass of the C quantum has been renormalized away by choosing the zero of energy appropriately. We also assume that we are always in the rest frame of the A quantum. This is not always a justifiable assumption unless we let these modes be 'infinitely heavy'. Incorporating the momenta carried by these discrete modes and including the recoil of A on emitting the Θ quantum does not change the essential behaviour of the system and is therefore avoided in the interest of clarity. To see how to include the momenta of these states, see [45].

Constants of motion other than H can be identified for the model which separates the Hilbert space of the system into orthogonal sectors that are preserved by the Hamiltonian. This introduces further simplifications to the problem of solving for the eigenstates of H. These constants are

$$N_1 = A^\dagger A + \int_0^\infty \mathrm{d}\omega\, \theta^\dagger(\omega)\theta(\omega) + C^\dagger C,$$

$$N_2 = \int_0^\infty \mathrm{d}\omega\, \theta^\dagger(\omega)\theta(\omega) + \int_0^\infty \mathrm{d}\nu\, \varphi^\dagger(\nu)\varphi(\nu),$$

$$N_3 = A^\dagger A + B^\dagger B.$$

The vacuum sector ($N_1 = N_2 = N_3 = 0$) has no particles in it. There is a one particle sector ($N_1 = N_3 = 1, N_2 = 0$) containing a single quantum of the B or the C field or a single stable quantum of the A field. The sector we are interested in is the one that contains a single *unstable* quantum of the A field together with a $|B\Theta\rangle$ and a $|BC\Phi\rangle$ ($N_1 = N_2 = N_3 = 1$). The $|A\rangle$ can decay into a B and a Θ. The Θ in turn can produce a C and a Φ. In this sector the states $|A\rangle$, $|B\Theta(\omega)\rangle$ and $|BC\Phi(\nu)\rangle$ are all coupled together. In the orthonormal basis furnished by the eigenstates of H_0, $\{|A\rangle, |B\Theta(\omega)\rangle, |BC\Phi(\nu)\rangle\}$ a generic state can be denoted by the vector

$$\Psi = \begin{pmatrix} \langle A|\Psi\rangle \\ \langle B\Theta|\Psi\rangle \\ \langle BC\Phi|\Psi\rangle \end{pmatrix} = \begin{pmatrix} \eta \\ \phi(\omega) \\ \psi^{(\omega)}(\nu) \end{pmatrix}. \tag{9}$$

The superscript label ω in the last component of the wavefunction is to show the dependence of the state on the motion (if any) of the Θ particle from which the Φ quantum was created. In the discussion that follows we will be ignoring this dependence for simplifying the calculations. The detector is assumed to be sensitive to quanta of the Θ field corresponding to a range of energies, $\omega_1 \leqslant \omega \leqslant \omega_2$, which is controlled by the function $G(\omega, \nu)$ in the Hamiltonian.

The Hamiltonian corresponding to this sector can be written in matrix form in the eigenbasis of H_0 as

$$H = \begin{pmatrix} m_A & f^*(\omega') & 0 \\ f(\omega) & (m_B + \omega)\delta(\omega - \omega') & G^*(\omega, \nu') \\ 0 & G(\omega', \nu)\delta(\omega' - \omega) & (m_B + \nu)\delta(\nu - \nu') \end{pmatrix}. \tag{10}$$

Note that some of the indices of the matrix above are continuous variables (ω and ν) and so this form of H should be treated as a concise representation of an operator rather than as a bona fide matrix. When the matrix acts on a column vector such as the one in equation (9) the primed variables are to be integrated over. Phase space factors (density of states) such as $\sqrt{\omega}$ and $\sqrt{\nu}$ that appear in the integrals and other constants are assumed to be absorbed into the functions $f(\omega)$ and $G(\omega, \nu)$ for the sake of keeping the mathematical development transparent.

2.3. Eigenstates of the Hamiltonian

The eigenvalue problem

$$H\Psi_\Lambda = \Lambda\Psi_\Lambda \tag{11}$$

leads to the following three coupled integral equations:

$$(\Lambda - m_A)\eta_\Lambda = \int_0^\infty \mathrm{d}\omega' f^*(\omega')\phi_\Lambda(\omega'), \tag{12}$$

$$(\Lambda - m_B - \omega)\phi_\Lambda(\omega) = f(\omega)\eta_\Lambda + \int_0^\infty \mathrm{d}\nu' G^*(\omega, \nu')\psi_\Lambda^{(\omega)}(\nu'), \tag{13}$$

$$(\Lambda - m_B - \nu)\psi_\Lambda^{(\omega)}(\nu) = \int_0^\infty \mathrm{d}\omega' G(\omega', \nu)\delta(\omega' - \omega)\phi_\Lambda(\omega'). \tag{14}$$

These three equations can be simultaneously solved in closed form. Starting from equation (14) we can solve for $\psi_\Lambda^{(\omega)}(\nu)$ as

$$\psi_\Lambda^{(\omega)}(\nu) = \frac{G(\omega, \nu)\phi_\Lambda(\omega)}{\Lambda - m_B - \nu + \mathrm{i}\epsilon} + e\delta(\Lambda - m_B - \nu)\delta(\nu - \omega). \tag{15}$$

The singular contribution to $\psi_\Lambda^{(\omega)}(\nu)$ when $\Lambda = m_B + \nu$ is written down separately in the second term in the above expression. This choice corresponds to a wavefunction with a *plane wave* contribution in the $|BC\Phi\rangle$ part. In the language of scattering theory the eigenstate of H that we are considering is an *out-state* which appears at infinity as a $|BC\Phi\rangle$. This is not the only choice of asymptotic boundary conditions that we can make. The other choice corresponds to having a plane wave contribution in the $|B\Theta\rangle$ part. This possibility is considered later on and the interpretation associated with either choice discussed. In the second term in equation (15), the factor $\delta(\omega - \nu)$ comes out of the requirement of energy conservation. It makes sure that the Φ quantum and the Θ quantum, from which the Φ was created, have exactly the same energy. This must be so mainly because we chose the mass of C to be the zero in our energy scale. The normalization constant e will turn out to be unity. Using (15) in equation (13) we obtain

$$\beta(\Lambda + \mathrm{i}\epsilon, \omega)\phi_\Lambda(\omega) = f(\omega)\eta_\Lambda + eG^*(\omega, \Lambda - m_B)\delta(\Lambda - m_B - \omega) \tag{16}$$

where

$$\beta(z, \omega) = z - m_B - \omega - \int_0^\infty \mathrm{d}\nu' \frac{|G(\omega, \nu')|^2}{z - m_B - \nu'} \tag{17}$$

is a real analytic function of z, analytic in the z-plane cut along the real axis from 0 to ∞. Therefore,

$$\phi_\Lambda(\omega) = \frac{f(\omega)}{\beta(\Lambda + \mathrm{i}\epsilon, \omega)}\eta_\Lambda + \frac{eG^*(\omega, \Lambda - m_B)}{\beta(\Lambda + \mathrm{i}\epsilon, \omega)}\delta(\Lambda - m_B - \omega). \tag{18}$$

Substituting this expression for $\phi_\Lambda(\omega)$ in (12) we can solve for η_Λ as

$$\eta_\Lambda = \frac{eG^*(\Lambda - m_B, \Lambda - m_B) f^*(\Lambda - m_B)}{\beta(\Lambda + \mathrm{i}\epsilon, \Lambda - m_B)\alpha(\Lambda + \mathrm{i}\epsilon)} \tag{19}$$

where

$$\alpha(z) = z - m_A - \int_0^\infty \mathrm{d}\omega' \frac{|f(\omega')|^2}{\beta(z, \omega')}. \tag{20}$$

Finally, applying the normalization condition, one can show that $e = 1$ (see appendix A).

We now have one set of solutions of the model given by

$$\Psi_\Lambda^{(1)} = \begin{pmatrix} \frac{G^*(\Lambda - m_B, \Lambda - m_B) f^*(\Lambda - m_B)}{\beta(\Lambda + \mathrm{i}\epsilon, \Lambda - m_B)\alpha(\Lambda + \mathrm{i}\epsilon)} \\ \frac{f(\omega)}{\beta(\Lambda + \mathrm{i}\epsilon, \omega)}\eta_\Lambda + \frac{G^*(\omega, \Lambda - m_B)}{\beta(\Lambda + \mathrm{i}\epsilon, \omega)}\delta(\Lambda - m_B - \omega) \\ \frac{G(\omega, \nu)\phi_\Lambda(\omega)}{\Lambda - m_B - \nu + \mathrm{i}\epsilon} + \delta(\Lambda - m_B - \nu)\delta(\nu - \omega) \end{pmatrix}. \tag{21}$$

The superscript in $\Psi_\Lambda^{(1)}$ indicates that there is another possible set of eigenstates to the Hamiltonian. To obtain these solutions, instead of equation (15) we choose

$$\psi_\Lambda^{(\omega)}(\nu) = \frac{G(\omega, \nu)\phi_\Lambda(\omega)}{\Lambda - m_B - \nu + \mathrm{i}\epsilon}, \tag{22}$$

with no plane wave contribution in the $|BC\Phi\rangle$ part of the wavefunction. This leads to

$$\phi_\Lambda(\omega) = \frac{f(\omega)}{\beta(\Lambda + \mathrm{i}\epsilon, \omega)}\eta_\Lambda + \tilde{e}_\Lambda \delta(\Lambda - m_B - \mathcal{K}_\Lambda - \omega). \tag{23}$$

A plane wave contribution to $\phi_\Lambda(\omega)$ can appear at an energy ω corresponding to the zero of the function $\beta(z, \omega)$. To solve

$$\beta(z, \omega) = z - m_B - \omega - \int_0^\infty \mathrm{d}\nu' \frac{|G(\omega, \nu')|^2}{z - m_B - \nu'} = 0$$

we make an approximation that the zero of $\beta(z, \omega)$ lies close to $\omega = z - m_B$. Using this approximation we find that the zero is at $\omega = z - m_B - \mathcal{K}_z$ where

$$\mathcal{K}_z = \int_0^\infty \mathrm{d}\nu' \frac{|G(z - m_B, \nu')|^2}{z - m_B - \nu'}. \tag{24}$$

Using (23) we get

$$\eta_\Lambda = \frac{\tilde{e}_\Lambda f^*(\Lambda - m_B - \mathcal{K}_\Lambda)}{\alpha(\Lambda + \mathrm{i}\epsilon)}. \tag{25}$$

The normalization is (see appendix A) $\tilde{e}_z = (\beta_z')^{-1/2}$ where

$$\beta_z' = \frac{\mathrm{d}}{\mathrm{d}z}\beta(z, \omega)\bigg|_{\omega = z - m_B - \mathcal{K}_z}.$$

Thus we have a second set of eigenstates of H belonging to the same sector as $|\Psi^{(1)}\rangle$ corresponding to out-states which asymptotically become a $|B\Theta\rangle$ plane wave given by

$$\Psi_\Lambda^{(2)} = \begin{pmatrix} \frac{1}{\sqrt{\beta_\Lambda'}} \frac{f^*(\Lambda - m_B - \mathcal{K}_\Lambda)}{\alpha(\Lambda + \mathrm{i}\epsilon)} \\ \frac{f(\omega)}{\beta(\Lambda + \mathrm{i}\epsilon, \omega)}\eta_\Lambda + \frac{1}{\sqrt{\beta_\Lambda'}}\delta(\Lambda - m_B - \mathcal{K}_\Lambda - \omega) \\ \frac{G(\omega, \nu)\phi_\Lambda(\omega)}{\Lambda - m_B - \nu + \mathrm{i}\epsilon} \end{pmatrix}. \tag{26}$$

2.4. How to use the solutions

What is relevant about the model in our investigation of the effect of repeated indirect measurements on an unstable quantum system are the following.

(i) The model provides explicit and exact solutions for the case in which we start with an unstable state $|A\rangle$ which decays into the combination $|B\Theta\rangle$. The $|B\Theta\rangle$ state in turn leads to the production of a new state $|BC\Phi\rangle$. The production of the $|\Phi\rangle$ quantum is interpreted as a pre-measurement.

(ii) With the exact wavefunctions available for the eigenstates of H we can compute the time evolution of the state $|A\rangle$ explicitly.

(iii) If we consider only the process $A \rightleftharpoons B\theta$ of the model, then in the sector we are considering, the Hamiltonian

$$H_{AB\Theta} = \begin{pmatrix} m_A & f^*(\omega') \\ f(\omega) & (m_B + \omega)\delta(\omega - \omega') \end{pmatrix} \tag{27}$$

is identical to the V–θ sector of the Friedrichs–Lee model [46–48]. The exact solutions of the Friedrichs–Lee model in this sector are well known and we can use these solutions to compare the behaviour of the unstable state $|A\rangle$ in the presence and in the absence of the 'detecting' excitation $|\Phi\rangle$.

2.5. Survival probability of $|A\rangle$

We are now in a position to compute the time evolution of a single, unstable quantum of the A field in the presence of the interactions that lead to the production of Φ as part of the pre-measurement. We start by computing the survival amplitude

$$\mathcal{A}(t) = \langle A|\, \mathrm{e}^{-\mathrm{i}Ht}|A\rangle. \tag{28}$$

Inserting complete sets of eigenstates of H

$$\mathcal{A}(t) = \mathcal{A}^{(1)}(t) + \mathcal{A}^{(2)}(t) \tag{29}$$

where

$$\mathcal{A}^{(1,2)}(t) = \int_0^\infty \mathrm{d}\Lambda \left|\left\langle A \,\middle|\, \Psi_\Lambda^{(1,2)}\right\rangle\right|^2 \mathrm{e}^{-\mathrm{i}\Lambda t}. \tag{30}$$

We have used the orthonormality of the eigenstates of H in equation (29) (see appendix A for proof). Using the solutions in equations (21) and (26) we obtain

$$\mathcal{A}^{(1)}(t) = \int_0^\infty \mathrm{d}\Lambda\, \mathrm{e}^{-\mathrm{i}\Lambda t} \left|\frac{G^*(\Lambda - m_B, \Lambda - m_B)}{\beta(\Lambda + \mathrm{i}\epsilon, \Lambda - m_B)}\right|^2 \times \left|\frac{f^*(\Lambda - m_B)}{\alpha(\Lambda + \mathrm{i}\epsilon)}\right|^2 \tag{31}$$

and

$$\mathcal{A}^{(2)}(t) = \int_0^\infty \mathrm{d}\Lambda\, \mathrm{e}^{-\mathrm{i}\Lambda t} \left|\frac{1}{\sqrt{\beta'_\Lambda}}\right|^2 \times \left|\frac{f^*(\Lambda - m_B - \mathcal{K}_\Lambda)}{\alpha(\Lambda + \mathrm{i}\epsilon)}\right|^2. \tag{32}$$

Before proceeding to investigate the behaviour of the survival probability $P(t) = |\mathcal{A}(t)|^2$ it is instructive to look at the evolution of the unstable state $|A\rangle$ in the absence of the coupling with the detector modes. This will give us an indication of how the indirect pre-measurement modifies the time evolution of $|A\rangle$ and also how to choose the nature of the detection process in such a way that we can obtain the Zeno effect.

3. Evolution of the unmeasured system

In the absence of the process $B\Theta \rightleftharpoons BC\Phi$ the model we are considering is identical to the V–Θ sector of the Friedrichs–Lee model which contains three interacting fields, V, N and Θ. Relabelling the fields A, B and Θ for comparison with the results of the previous section and using the Hamiltonian $H_{AB\theta}$ in (27) the eigenstates of the Friedrichs–Lee model are

$$\zeta_\Lambda = \begin{pmatrix} \langle A|\zeta_\Lambda\rangle \\ \langle B\Theta(\omega)|\zeta_\Lambda\rangle \end{pmatrix} = \begin{pmatrix} \frac{f^*(\Lambda - m_B)}{\gamma(\Lambda + \mathrm{i}\epsilon)} \\ \delta(\Lambda - m_B - \omega) + \frac{f(\omega) f^*(\Lambda - m_B)}{\gamma(\Lambda + \mathrm{i}\epsilon)(\Lambda - m_B - \omega + \mathrm{i}\epsilon)} \end{pmatrix} \tag{33}$$

where

$$\gamma(z) = z - m_A - \int_0^\infty \mathrm{d}\omega' \frac{|f(\omega')|^2}{z - m_B - \omega'}.$$

The survival amplitude of the unstable state $|A\rangle$ in the Friedrichs–Lee model is

$$\begin{aligned} \widetilde{\mathcal{A}}(t) &= \int_0^\infty \mathrm{d}\Lambda\, \mathrm{e}^{-\mathrm{i}\Lambda t} |\langle A|\zeta_\Lambda\rangle|^2 \\ &= \int_0^\infty \mathrm{d}\Lambda\, \mathrm{e}^{-\mathrm{i}\Lambda t} \left| \frac{f^*(\Lambda - m_B)}{\gamma(\Lambda + \mathrm{i}\epsilon)} \right|^2. \end{aligned} \tag{34}$$

To be able to compute the survival probability, $P(t) = |\widetilde{\mathcal{A}}(t)|^2$, of the unstable $|A\rangle$ state in the Friedrichs–Lee model all we have to do is to choose an appropriate form factor $f(\omega)$. The results from a particular choice of the form factor are given below for comparison with the time evolution of the unstable state in the full model.

3.1. Numerical investigations: the unmeasured system

We choose $f(\omega)$ to have the form

$$f(\omega) = \frac{c\mu^2\sqrt{\omega}}{(\omega - \omega_0)^2 + \mu^2}; \qquad 0 \leqslant \omega \leqslant +\infty. \tag{35}$$

This is a Lorentzian line shape with the extra factor of $\sqrt{\omega}$ in the numerator coming from the phase space contribution due to our choice of working with the energy variable rather than the momentum. The constant c controls the magnitude of the interaction. All other constants, including powers of π, are absorbed into c. The line width of the interaction is determined by μ while ω_0 determines where its peak is located.

We work with scaled units where ω, ω_0 and μ really stand for multiples of a typical energy scale ω_T that is appropriate for the specific physical system that we are interested in. We refer the reader to [34] for a concise presentation of possible realistic choices and ranges for these variables.

For this choice of the form factor the Friedrichs–Lee model propagator $\gamma(z)$ can be computed in closed form as

$$\begin{aligned} \gamma(z) &= z - m_A - c^2\mu^4 \int_0^\infty \mathrm{d}\omega' \frac{\omega'}{[(\omega' - \omega_0)^2 + \mu^2]^2 (z - \omega')} \\ &= z - m_A - \frac{c^2\mu^2(z - \omega_0)}{2[(z - \omega_0)^2 + \mu^2]} \\ &\quad - \frac{c^2\mu}{4}\left(\pi + 2\tan^{-1}\left(\frac{\omega_0}{\mu}\right)\right)\left(\frac{z(z - \omega_0)\left(1 + \frac{2\mu^2}{(z-\omega_0)^2+\mu^2}\right)}{(z - \omega_0)^2 + \mu^2} - 1\right) \\ &\quad - \frac{c^2\mu^3 z}{4[(z - \omega_0)^2 + \mu^2]^2} \log\left[\frac{z^2}{\mu^2 + \omega_0^2}\right]. \end{aligned} \tag{36}$$

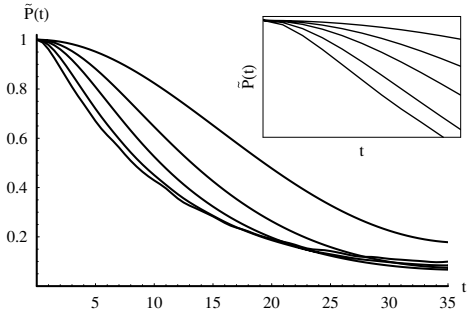

Figure 1. Survival probability $\widetilde{P}(t)$ of the unstable state in the Friedrichs–Lee model for $\mu = 0.1, 0.3, 0.5, 1$ and 2 with $\omega_0 = m_A = 2, c = 0.1$ and $\epsilon = 0.05$. The steepest curve corresponds to $\mu = 2$ and for lower values of μ the survival probability decays slower. The inset shows the short time behaviour ($0 \leqslant t \leqslant 5$).

We use the propagator with $z = \Lambda + \mathrm{i}\epsilon$ to compute the survival probability, $\widetilde{P}(t) = |\widetilde{\mathcal{A}}(t)|^2$, for the unstable $|A\rangle$ state in the Friedrichs–Lee model for different choices of the parameters in the form factor $f(\omega)$.

The following conventions and simplifications have been used to perform the numerical computations to obtain $\widetilde{P}(t)$. Since $|f(\omega)|^2$ is the discontinuity of the denominator function across the branch cut that lies along the positive real axis, it is always true (see [48]) that

$$\begin{aligned}\widetilde{P}(0) &= \lim_{\epsilon\to 0}\int_0^\infty \mathrm{d}\Lambda \frac{|f^*(\Lambda - m_B)|^2}{\gamma(\Lambda+\mathrm{i}\epsilon)\gamma(\Lambda-\mathrm{i}\epsilon)} \\ &= \lim_{\epsilon\to 0} -\frac{1}{2\pi i}\int_0^\infty \mathrm{d}\Lambda \frac{\gamma(\Lambda+\mathrm{i}\epsilon)-\gamma(\Lambda-\mathrm{i}\epsilon)}{\gamma(\Lambda+\mathrm{i}\epsilon)\gamma(\Lambda-\mathrm{i}\epsilon)} \\ &= \lim_{\epsilon\to 0} -\frac{1}{2\pi \mathrm{i}}\oint_C \mathrm{d}z \frac{1}{\gamma(z)} = 1. \end{aligned} \tag{37}$$

Due to the limitations of the numerical computations, $\widetilde{P}(0)$ does not come out to be exactly equal to 1. In such cases we re-normalize the computed survival probability to $\widetilde{P}(t)/\widetilde{P}(0)$ as long as $\widetilde{P}(0)$ is not too far from being equal to 1 (at most 10%). Since equation (37) is an exact, analytical result we are assured that $\widetilde{P}(0) \neq 1$ in the numerical investigations is not a consequence of real effects like wavefunction re-normalization which might have been overlooked. We have also verified that $\widetilde{P}(0)$ converges to unity if we increase the accuracy of the numerical integrations. In what follows we are interested only in comparing the *forms* of the graphs of various survival probabilities that we compute and so we use a uniform, modest numerical accuracy for all the computations. To simplify matters further, in what follows, we have chosen the mass of the B particle m_B to be identically zero. In our model this means that both B and C have the same mass. Only the mass m_A of the decaying state $|A\rangle$ has a role in determining the *shape* of the graph of $\widetilde{P}(t)$.

In figure 1 we plot the survival probability as a function of time for various values of μ keeping all the other parameters constant. The peak of the form factor coincides with the mass of A (both are equal to 2 in arbitrary scaled units) in the plots in figure 1. The interaction is a resonant one. Accuracy of the numerical computations performed using *Mathematica* limits the value of ϵ to be around 0.05.

We see that as $f(\omega)$ becomes wider with increasing values of μ the decay rate $\tilde{\widetilde{P}}(t)$ increases. We also note that the initial quadratic regime in the decay of the survival probability which facilitates the occurrence of the Zeno effect gets shortened as μ increases. The support of the wavefunction of the unstable state $|A\rangle$ on the eigenstates $|\zeta_\Lambda\rangle$ of $H_{AB\Theta}$, given by

the function $|\langle A|\zeta_\Lambda\rangle|^2$, increases when μ increases. The survival amplitude of $|A\rangle$ is the Fourier transform of $|\langle A|\zeta_\Lambda\rangle|^2$. When $|\langle A|\zeta_\Lambda\rangle|^2$ becomes a wider function, the survival amplitude becomes a narrower, steeper function. The modification of the behaviour of the survival amplitude of $|A\rangle$, especially at short times, brought about by changing $f(\omega)$ becomes significant when we look for the effect of the indirect pre-measurements on the decaying states. The results presented here on the Friedrichs–Lee model are well known. We reproduce the basic points here as a prelude to how the indirect pre-measurements can be tuned to modify the decay rate of the observed system. The modified decay rates in turn can be used to produce the quantum Zeno and possibly the anti-Zeno effect.

4. Zeno and anti-Zeno effects from indirect pre-measurements

Comparison of equations (29), (31) and (32) with equation (34) shows that the behaviour of the survival amplitude of the unstable state $|A\rangle$ is modified in three qualitatively different ways when the indirect pre-measurements are introduced into the system.

(i) The most obvious difference is that when the pre-measurements are present, $|A\rangle$ can decay through two distinct channels with amplitudes given by $\mathcal{A}^{(1)}(t)$ and $\mathcal{A}^{(2)}(t)$. In the Friedrichs–Lee model there is only one available channel with amplitude $\widetilde{A}(t)$. Only one of the channels in the evolution with the pre-measurements leads to the production of a detector excitation $|\Phi\rangle$ asymptotically. This presents us with the question of how to interpret the presence of the two channels in relation to what is being measured of the decaying state. A discussion of this issue is included in section 4.1.

(ii) The denominator function (propagator) $\gamma(z)$ corresponding to the process $A \rightleftharpoons B\Theta$ in the unmeasured case is modified to $\alpha(z)$ when the pre-measurements are introduced. If the function $\mathcal{K}(z)$ defined in equation (24) is small so that $\beta(z,\omega) \sim z - m_B - \omega$ then $\alpha(z)$ is approximately the same as $\gamma(z)$. In our numerical investigations we choose the parameters and form factors such that $\alpha(z) \sim \gamma(z)$ so that we can isolate the effect of changing the shape and position of $G(\omega,\nu)$ on the behaviour of the pre-measured system while ignoring the influence of changes to the denominator function.

(iii) With the assumption that the modifications to the denominator function are minimal we see that the integrands in (31) and (32) contain a factor $|f^*/\alpha|^2$ that is identical to the factor $|\langle A|\zeta_\Lambda\rangle|^2$ that appears in (34). We can therefore view the amplitudes $\mathcal{A}^{(1)}(t)$ and $\mathcal{A}^{(2)}(t)$ as Fourier transforms of the overlap $|\langle A|\zeta_\Lambda\rangle|^2$ of the unmeasured case modified by the multiplicative factors $h^{(1)}(\Lambda)$ and $h^{(2)}(\Lambda)$, respectively, where

$$h^{(1)}(\Lambda) = \left|\frac{G^*(\Lambda - m_B, \Lambda - m_B)}{\beta(\Lambda + \mathrm{i}\epsilon, \Lambda - m_B)}\right|^2 \tag{38}$$

and

$$h^{(2)}(\Lambda) = \left|\frac{1}{\sqrt{\beta'_\Lambda}}\right|^2. \tag{39}$$

The function $h^{(1)}(\Lambda)$ depends explicitly on $G(\omega,\nu)$ that controls the 'detecting' process $B\Theta \rightleftharpoons BC\Phi$. By changing the nature of the detector we are therefore able to change the manner in which $|A\rangle$ decays. The modifying function for the second channel, $h^{(2)}(\Lambda)$, also has an implicit dependence on $G(\omega,\nu)$ through β' although this dependence is very weak and not easy to exploit. Before we can figure out how to choose $G(\omega,\nu)$ so as to generate suppression or enhancement of the decay rate of the pre-measured system in relation to the unmeasured case we need to understand how to interpret the two channels through which the decay of the pre-measured system can occur.

4.1. A note on interpretation

Only the decay of $|A\rangle$ through the first channel with amplitude $\mathcal{A}^{(1)}(t)$ asymptotically leads to the production of a $|\Phi\rangle$ quantum. Since it is the excitation of the Φ field that is transformed into a classical signal during the non-unitary part of the measurement process we assume that only the decay through this channel is ever detected. If the initial state decays through the second channel, there still is an excitation of the Φ field with an amplitude given by the $\psi^{(\omega)}_{\Lambda}(\nu)$ component of $\Psi^{(2)}_{\Lambda}$. Since $\psi^{(\omega)}_{\Lambda}(\nu)$ in the case of the second channel is not a singular function in energy and momentum space, we assume that this excitation exists only for a finite time with a finite extent in configuration space and dies away without propagating to infinity. A detector with a sufficiently fast response time located close to the decaying A particle can in principle catch this signal and produce a macroscopic effect out of it. We assume that this is not the case here. *The part of the detector that is responsible for extracting a classical signal out of the excitation of the Φ field that is created by the decay products of $|A\rangle$ is sensitive only to states of the type $\Psi^{(1)}_{\Lambda}$ which asymptotically become $|BC\Phi\rangle$ states.*

With this picture in mind we interpret $P^{(1)}(t) = |\mathcal{A}^{(1)}(t)|^2$ as the probability that the detector 'clicks' when $|A\rangle$ decays. $P^{(2)}(t) = |\mathcal{A}^{(2)}(t)|^2$ is the probability that the detector fails to notice given that $|A\rangle$ has indeed decayed. The actual survival probability of the state $|A\rangle$ in the dynamical system that includes the pre-measurement is $P(t) = |\mathcal{A}^{(1)}(t) + \mathcal{A}^{(2)}(t)|^2$. Note that $P(t) \neq P^{(1)}(t) + P^{(2)}(t)$.

According to our choice of the function $G(\omega, \nu)$ we can make the decay through one of the channels a substantially dominant process thereby making $P(t) \sim P^{(1)}(t)$ or $P(t) \sim P^{(2)}(t)$ as the case may be. The former case is when the pre-measurement has a significant effect on the decay of $|A\rangle$ and the latter is when the detector is, for most practical purposes, decoupled from the quantum system. A third and interesting possibility is when the two amplitudes $\mathcal{A}^{(1)}(t)$ and $\mathcal{A}^{(2)}(t)$ are comparable and can interfere with each other making $P(t)$ different from both $P^{(1)}(t)$ and $P^{(2)}(t)$.

An important question as far as interpretation of the numerical results is the meaning of the '*probability of detection*' $P^{(1)}(t)$ when it is small compared to $P^{(2)}(t)$ (or vice versa). If one were to plot both $P^{(1)}(t)$ and $P^{(2)}(t)$ on the same graph, $P^{(1)}(t)$ might start at a much lower point than $P^{(2)}(t)$ if $P^{(1)}(0) \ll P^{(2)}(0)$. On the other hand, *probabilities themselves are physically measurable only when viewed as frequencies* and so it makes more sense to compare $P^{(1)}(t)/P^{(1)}(0)$ and $P^{(2)}(t)/P^{(2)}(0)$ with $P(0) = P^{(1)}(0) + P^{(2)}(0) = 1$. This could be viewed as a comparison of the *decay rates* through the two different channels rather than as a comparison of the raw survival probabilities. The graph of $P^{(1)}(t)/P^{(1)}(0)$ would then correspond to the decay curve that an experimenter would draw from detector count data under the assumption that initially the sample consisted entirely of non-decayed $|A\rangle$ states and also that the detector is one hundred per cent efficient.

4.2. Numerical investigations: the pre-measured system

The first step is to choose an appropriate *detector function* $G(\omega, \nu)$ that controls the pre-measurement interaction $B\Theta \rightleftharpoons BC\Phi$. Since we are primarily interested in investigating the effects of the height, width and location of $G(\omega, \nu)$ on the decay of $|A\rangle$ we choose G to be a square step given by

$$G(\omega, \nu) = \begin{cases} \delta & a \leqslant \omega, \nu \leqslant b \\ 0 & \text{otherwise} \end{cases} \qquad 0 \leqslant \omega, \nu \leqslant \infty \tag{40}$$

where δ is the height of the step and $L \equiv b - a$ is its width. The location of the step is controlled by changing a and b. This is not a very realistic detector function but we use it in

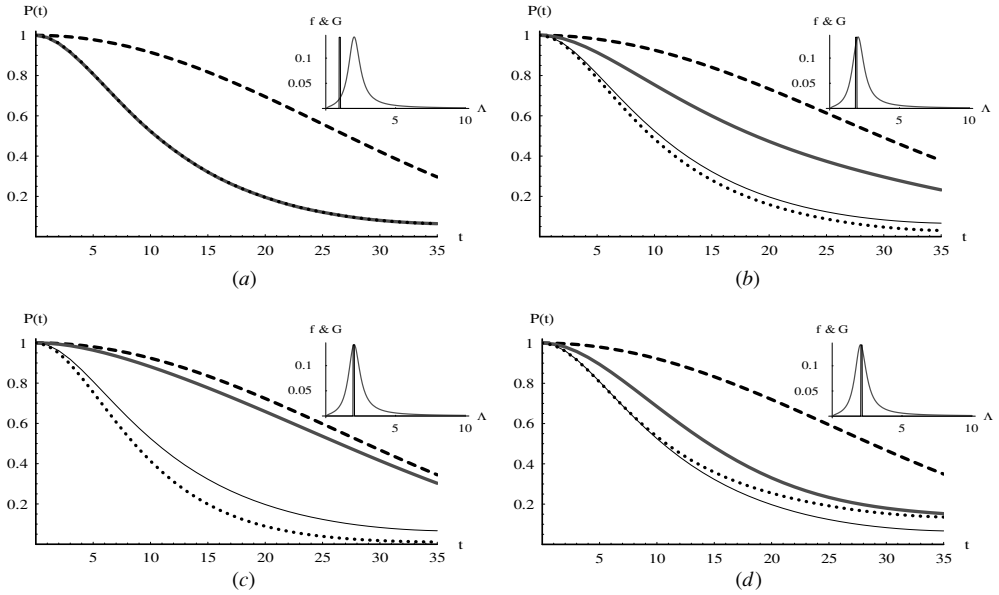

Figure 2. Sampling the decay with a narrow measurement window in frequency space ($L = 0.1 < \mu = 0.5$): the form factors $f(\omega)$ and $G(\omega, \nu)$ are shown in insets. The dashed line is $P^{(1)}(t)$ which is the 'observed' decay. The dotted line is $P^{(2)}(t)$, the part of the decay amplitude that is not detected. The thin line is $\widetilde{P}(t)$ while the thick solid line is the real decay of the system, $P(t)$. The centres of the detector function are at 1, 1.9, 2 and 2.1 in (*a*), (*b*), (*c*) and (*d*) respectively. If the centre of the detector function is located at higher values of Λ, the plots obtained are similar to (*a*).

the interest of significantly simplifying the numerical calculations without compromising on the qualitative features of the dynamics.

Using this $G(\omega, \nu)$ we can now compute the actual survival probability, $P(t)$ of $|A\rangle$, the 'measured' survival probability $P^{(1)}(t)/P^{(1)}(0)$ and the component $P^{(2)}(t)/P^{(2)}(0)$ that the detector fails to see. All three can be compared with survival probability $\widetilde{P}(t) = |\widetilde{\mathcal{A}}(t)|^2$ of the same system that is not subject to the pre-measurement process. In the following discussion we denote $P^{(1)}(t)/P^{(1)}(0)$ just as $P^{(1)}(t)$ and $P^{(2)}(t)/P^{(2)}(0)$ as $P^{(2)}(t)$. In all the computations we keep the form factor $f(\omega)$ the same with parameter values $\mu = 0.5$ and $\omega_0 = m_A = 2$. In this paper we also keep the height of $G(\omega, \nu)$ a constant and we choose it to be the same as the peak height of $f(\omega)$. Here we focus only on the effect of the width and the location of $G(\omega, \nu)$ has on the way the unstable state $|A\rangle$ decays.

4.2.1. A narrow detector function. The width of the modifying function $h^{(1)}(\Lambda)$ in the integral that defines $\mathcal{A}^{(1)}(t)$ is equal to the width of $G(\Lambda, \Lambda)$. From our analysis of the unmeasured system we recognize that if $\left|\left\langle A \mid \Psi_{\Lambda}^{(1,2)}\right\rangle\right|^2$ has a very narrow support in the energy domain then the corresponding decay of $|A\rangle$ through that channel will be very slow. To take advantage of this observation we make the width L of the detector function much smaller than that of $f(\omega)$. If we can now make the decay into the first channel the dominant process as well we will be able to significantly suppress the rate of decay of $|A\rangle$ just by virtue of the pre-measurements being present. We look only at the effect of the location of the centre of $G(\omega, \nu)$ on the three probabilities $P^{(1)}(t)$, $P^{(2)}(t)$ and $P(t)$ that are of interest to us. The result is summarized in figure 2.

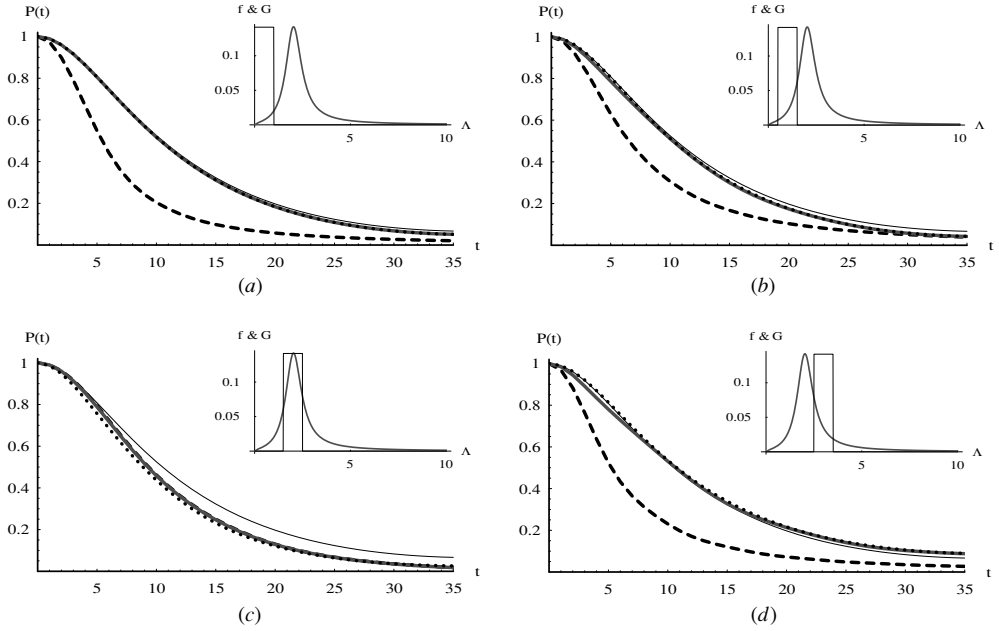

Figure 3. Sampling the decay with a wide measurement window in frequency space ($L = 1 > \mu = 0.5$): the form factors $f(\omega)$ and $G(\omega, \nu)$ are shown in insets. The dashed line is $P^{(1)}(t)$ which is the 'observed' decay. The dotted line is $P^{(2)}(t)$, the part of the decay amplitude that is not detected. The thin line is $\widetilde{P}(t)$ and the thick solid line is the real decay of the system, $P(t)$. The centres of the detector function are at 0.5, 1, 2 and 3 in (*a*), (*b*), (*c*) and (*d*) respectively. If the centres are at larger values of Λ, the plots obtained are similar to (*a*).

From figure 2 we can come to the following conclusions: if the detector is sampled using a very narrow window in frequency space, the *observed* decay rate $\dot{P}^{(1)}(t)$ will always be suppressed relative to both the real decay rate $\dot{P}(t)$ and the decay rate $\dot{\widetilde{P}}(t)$ of the unmeasured system. If the measurement is made at frequencies that are far away from the peak of the line shape $f(\omega)$ of the decay process, then the observed rate will not have much connection with what is actually happening. This is illustrated in figure 2(*a*). The dominant process in this instance is the decay through the second channel which proceeds without being detected; this is clearly not a good way of setting up our detector. If we do set up the detector to observe the decay at energies near the peak of $f(\omega)$, we see that the dominant process decays through the observed channel. So the graph of $P(t)$ is very close to that of $P^{(1)}(t)$ and there is a real suppression of the decay rate due to the presence of the pre-measurement see figures 2(*b*), (*c*) and (*d*). In other words, there is a real modification of the effective decay rate $\gamma(t)$ of the pre-measured system with respect to γ_0 of the unmeasured system. This makes it easier to find a τ such that $\gamma(\tau) < \gamma_0$ thereby facilitating the observation of the Zeno effect.

4.2.2. A wide detector function. Taking our cue from the fact that a narrow detector function can generate a real suppression of the decay rate of $|A\rangle$ one is tempted to think that if $G(\omega, \nu)$ is chosen to be wider than $f(\omega)$ it might lead to an enhancement in the decay rate which can then be exploited to obtain the anti-Zeno effect. The results of sampling the decay process with a wide detector function is given in figure 3. The observed decay rate $\dot{P}^{(1)}(t)$ is enhanced in comparison to the decay rate of the unmeasured system only when the detector function is located far from the peak of the form factor $f(\omega)$. When we place the centre of the wide

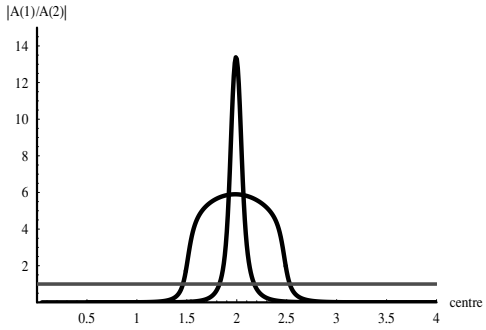

Figure 4. The relative importance of the measured and unmeasured amplitudes at time $t = 0$ as a function as the location of the centre of the detector function G. The sharp curve corresponds to the narrow detector function while the broad curve is for the wide detector function. The straight line is $|\mathcal{A}^{(1)}(t)/\mathcal{A}^{(2)}(t)| = 1$.

detector function in coincidence with the peak of the form factor both the observed and real decay become very similar to the behaviour of the unmeasured system as seen figure 3(c). Making the detector function wide does not change the effective decay rate $\gamma(t)$ of the pre-measured system. Only the observed part of the decay is modified. This means that the anti-Zeno effect, unlike the Zeno effect, cannot be obtained just by modulating the detector function. An apparent anti-Zeno effect can however be obtained. This possibility is discussed in section 6.

To check the consistency of the numerical calculations we computed the survival probabilities when $G(\omega, \nu)$ is very wide compared to $f(\omega)$ and captures the signals in all frequencies that are produced when $|A\rangle$ decays. We see that the observed, the actual and the unmeasured decay curves fall one on top of the other. Using a detector with such a wide frequency response we are therefore able to measure the actual evolution of the survival probability of $|A\rangle$ without having to worry about the pre-measurement modifying the dynamics in any significant manner.

4.3. Interference when the two amplitudes $\mathcal{A}^{(1)}(t)$ and $\mathcal{A}^{(2)}(t)$ are comparable

A third interesting possibility that we mentioned before is when $\mathcal{A}^{(1)}(t)$ and $\mathcal{A}^{(2)}(t)$ are comparable in magnitude and can interfere with each other making $P(t)$ quite different from both $P^{(1)}(t)$ and $P^{(2)}(t)$. The ratio of the two amplitudes at time $t = 0$ is plotted as a function of the location of the centre of the detector function in figure 4. The figure explains why the observed decay curve is almost the same as the real decay curve when the centre of the detector function coincides with the peak of $f(\omega)$. It also shows why a real enhancement of the decay rate is not possible when the detector function is wide compared to $f(\omega)$ and placed at the peak of $f(\omega)$ because when $G(\omega, \nu)$ is wide, $\mathcal{A}^{(1)}(t)$ never becomes overwhelmingly bigger in magnitude than $\mathcal{A}^{(2)}(t)$. This is not the case when the detector function is very narrow compared to $f(\omega)$. When it is narrow, placing its centre in coincidence with the peak of the line shape makes the slower decay through the detected channel the dominant process and therefore we are able to make the decay rate as small as we want just by using our control over $G(\omega, \nu)$.

From figure 4 we see that when the centre of the wide detector function is at 1.4 or 2.6 (in the arbitrary energy scale) or when the centre of the narrow detector function is at 1.8 or 2.2 the two amplitudes $\mathcal{A}^{(1)}(t)$ and $\mathcal{A}^{(2)}(t)$ are comparable. We expect them to interfere at these parameter ranges. This is seen in the plots of $P^{(1)}(t)$, $P^{(2)}(t)$ and $P(t)$ given in figures 5 and 6.

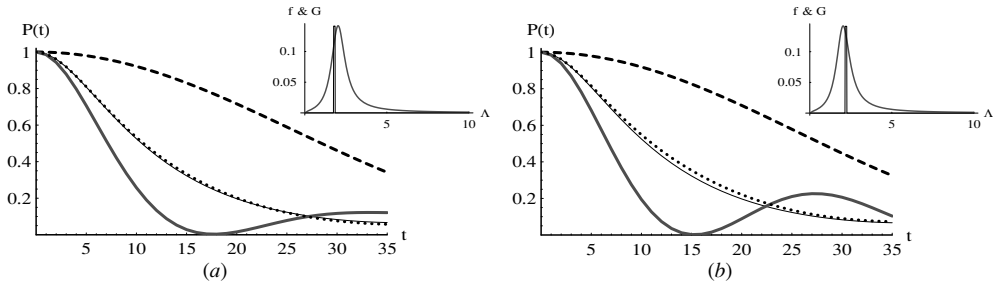

Figure 5. The two graphs on the right-hand side show $P^{(1)}(t)$ (dashed line), $P^{(2)}(t)$ (dotted line), $\widetilde{P}(t)$ (thin line) and $P(t)$ (thick solid line) when the measurement window is narrow ($L = 0.1$) and when centre of $G(\lambda, \lambda)$ is located at 1.8 and 2.2 in (a) and (b) respectively such that $|\mathcal{A}^{(1)}(0)/\mathcal{A}^{(2)}(0)| \simeq 1$. The form factors f and G are shown in insets.

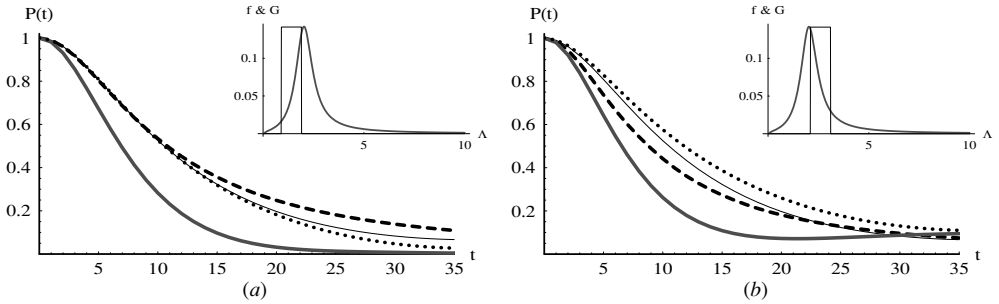

Figure 6. The two graphs on the right-hand side show $P^{(1)}(t)$ (dashed line), $P^{(2)}(t)$ (dotted line), $\widetilde{P}(t)$ (thin line) and $P(t)$ (thick solid line) when the measurement window is wide ($L = 1$) and when centre of $G(\lambda, \lambda)$ is located at 1.4 and 2.6 in (a) and (b) respectively such that $|\mathcal{A}^{(1)}(0)/\mathcal{A}^{(2)}(0)| \simeq 1$. The form factors f and G are shown in insets.

What is missing from the numerical investigations of the system with pre-measurements is the effect of the strength of the system–detector coupling δ on the dynamics. We plan to investigate this in a separate paper.

5. Repeated measurements

The model we have constructed deals entirely with the effects of a pre-measurement on the unstable state $|A\rangle$. So far we have not considered the effects of continuing with the measurement process to obtain a classical signal from the detector that indicates the decay of $|A\rangle$. The measurement process will most likely involve the destruction of the $|\Phi\rangle$ state that is produced in the pre-measurement leading to an amplified signal. We approximate this process by arbitrarily setting the last two components $\phi_\Lambda(\omega)$ and $\psi_\Lambda^{(\omega)}(\nu)$ of the time evolved state

$$|A(t)\rangle = \int_0^\infty \mathrm{d}\Lambda\, \mathrm{e}^{-\mathrm{i}\Lambda t}\left[\left\langle\Psi_\Lambda^{(1)}\middle|A\right\rangle\middle|\Psi_\Lambda^{(1)}\right\rangle + \left\langle\Psi_\Lambda^{(2)}\middle|A\right\rangle\middle|\Psi_\Lambda^{(2)}\right\rangle\Big]$$

to be zero to simulate the effect of a full measurement on the system. The state which starts out as $|A\rangle = (1, 0, 0)^T$, after a full measurement at $t = \tau$ becomes

$$|A\rangle^\tau = \begin{pmatrix} P^{(1)}(\tau) \\ 0 \\ 0 \end{pmatrix}; \qquad P^{(1)}(\tau) = \int_0^\tau \mathrm{d}\Lambda\, \mathrm{e}^{-\mathrm{i}\Lambda t}\left|\left\langle A\middle|\Psi_\Lambda^{(1)}\right\rangle\right|^2.$$

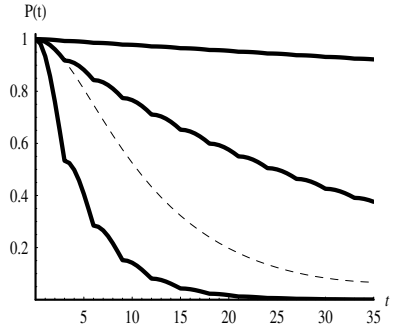

Figure 7. The behaviour of the survival probability with repeated measurements. The dashed line is the free evolution of the unmeasured system. The thick line in the middle is for the unmeasured system interrupted at intervals $\tau = 3$. The top curve is the measured survival probability $P^{(1)}(t)$ when pre-measurements with a narrow detection window ($L = 0.1$) is present. The lower curve is again the measured survival probability $P^{(1)}(t)$ when pre-measurement is done with a wide window ($L = 1$) with the peak of the detector function far away from the peak of $f(\omega)$.

$P^{(1)}(\tau)$, and not $P(\tau)$, appears in the expression for $|A\rangle^{\tau}$ because for the measurement to have happened we have to assume that the decay has occurred through the first channel and not the second one. To model repeated measurements we start the next time from $|A\rangle^{\tau}$ instead of $(1, 0, 0)^T$ and let it evolve again for τ units of time and so on. This gives us only the time evolution of the 'observed part' of the decay process under the influence of repeated measurements. We have seen earlier, though, that by choosing the detector function appropriately we can make the real behaviour of the decay curve come as close as we want to the behaviour of the observed part in some cases.

If $P(\tau) \sim P^{(1)}(\tau) < \widetilde{P}(\tau)$ then $[P^{(1)}(\tau)]^n < \widetilde{P}(t = n\tau)$ leading to a suppression of the decay rate of the repeatedly measured system compared to the decay rate of the unmeasured one (the Zeno effect). Moreover, we see that $[P^{(1)}(\tau)]^n < [\widetilde{P}(\tau)]^n$ indicating that not only is the Zeno effect possible, but also that the pre-measurements can be tuned to make it easier to see the Zeno effect. If, on the other hand $P^{(1)}(\tau) > \widetilde{P}(\tau)$ (a wide detector function placed away from the peak of $F(\omega)$) we can obtain the anti-Zeno effect. We cannot call this a real anti-Zeno effect that genuinely speeds up the decay of $|A\rangle$ because even if $P^{(1)}(\tau) > \widetilde{P}(\tau)$ for certain choices of the parameters, for these values the real evolution $P(\tau)$ is close to the unmeasured evolution $\widetilde{P}(\tau)$ rather than being close to what is 'detected'.

Interrupted evolution of $|A\rangle$ with and without pre-measurements is shown in figure 7. The unmeasured system is interrupted periodically after free evolution for $\tau = 3$ units. This is just before the survival probability curve becomes exponential. It is understood that to produce Zeno effect in a system without pre-measurements, it has to be interrupted at time intervals shorter than or equal to $\tau = 3$. When the pre-measurements are present we see that for the same interruption time, either a more pronounced Zeno effect or an apparent anti-Zeno effect is seen in the observed survival probability curve.

6. Conclusions

We have studied a model of indirect pre-measurements on an unstable quantum state $|A\rangle$. We see that the way the pre-measurements are performed can have an effect on the dynamics of the decaying state. If we have a detector that samples a narrow window in energy space for the decay products of $|A\rangle$ as in figure 2 then the presence of the detector can lead to a suppression

of the real decay rate of the state. This is a fascinating result because the detector does not actively measure the decaying state but rather waits to detect the products of the decay. The main difficulty in obtaining the Zeno effect is very often the lack of sufficient time resolution for the detector. The decaying state has to be locked into the initial non-exponential regime of its decay curve by interrupting it sufficiently frequently. Let us assume for a moment that the detectors that we have do not have sufficient temporal resolution to interrupt the evolution of the state $|A\rangle$ at sufficiently small time intervals when it is evolving freely. The observed decay curves $P^{(1)}(t)$ in figure 2 are quadratic for a longer time when the pre-measurements are performed on the state with a narrow detector window. This makes it easier to obtain the Zeno effect by repeating complete measurements when the pre-measurements modify the evolution of $|A\rangle$.

One has to be careful because we have the possibility of obtaining an apparent Zeno effect in addition to a real one. If one were to couple the decay products of $|A\rangle$ with the quantum part of the detector using a narrow energy window at energies far away from the peak of $f(\omega)$, then the observed suppression of the decay rate of $|A\rangle$ would merely be an illusory effect generated by the measurement process. In this case a lot of decay events would go undetected if we had started off with an ensemble of identical $|A\rangle$ states. We will then end up with an apparent suppression of the decay rate since only $P^{(1)}(t)$ is measured. The Zeno effect obtained by repeating the non-exponential part of the observed decay curve $P^{(1)}(t)$ has no connection with the real dynamics of the state in this case. If, on the other hand, we couple the system with the detector strongly by making the peak of the narrow detector function coincide with the peak of the resonance curve of the decay, we will be able to genuinely suppress the real decay rate of the measured system. By interrupting this modified decay process periodically through the completion of the measurement one can further enhance the suppression of the decay and get a true, full-fledged quantum Zeno effect. In other words what is important is that when the detector is sensitive to that narrow window in energy space to which it really should be sensitive to in order to be a 'good' detector, then the suppression of decay rate of $|A\rangle$ is a real effect.

The anti-Zeno effect also appears in our model but only as an apparent effect. From figure 3 we conclude that it is not possible to obtain a real anti-Zeno effect by just increasing the width of the detector function. An apparent anti-Zeno effect is possible though. If $G(\omega, \nu)$ is chosen so as to measure the system at energies away from the peak of $f(\omega)$, the observed decay curve $P^{(1)}(t)$ shows an enhancement of the decay rate compared to both the unmeasured evolution $\widetilde{P}(t)$ and also the real evolution $P(t)$ of system. Repeated application of such measurements will appear to speed up the decay as seen in figure 7. This apparent Zeno effect is in agreement with what is observed by Kofman and Kurizki in [9]. The anti-Zeno effect does appear in their analysis under similar conditions. The conclusion in [9] is that since a measurement of this sort is much easier to perform than the kind that leads to the Zeno effect, the anti-Zeno effect must be the more readily observable of the two. We point out that with our model also it is easier to obtain the anti-Zeno effect out of the enhancement of decay when a wide detector function is used. Our model suggests that the 'easily observable' anti-Zeno effect appears as an artefact of the way we perform the measurement and not as a real effect. When we do bring the wide detector function close to the peak of $f(\omega)$ with the hope of seeing a real speed-up of the decay, what happens instead is that $P^{(1)}(t)$ approaches both $P(t)$ and $\widetilde{P}(t)$ rather than $P(t)$ approaching $P^{(1)}(t)$. So in our model the anti-Zeno effect remains just a product of the way the detector is set up with no relation to the actual dynamics of the system under consideration.

There seems to be an enhancement of the real decay rate $\dot{P}(t)$ in both figures 5 and 6 but this enhancement is clearly not detectable using our detector since $P^{(1)}(t)$ remains

unchanged. We cannot get the anti-Zeno effect by measuring the system in the manner shown in figures 5 and 6. Moreover, the parameter ranges over which this effect can be created is very small and a generic detector is very unlikely to affect the system it is measuring in this particular manner.

The suppression of the decay rate of the unstable state due to the pre-measurements is an interesting phenomenon because a common roadblock in observing the Zeno effect is that the quantum system has to be observed at a frequency higher than that allowed by most detectors. Here we see that in the case of a pre-measured decaying state, the part of the detector that is responsible for interacting with the system can itself be chosen so that it suppresses the natural decay of the state being observed. This would mean that the process of measurement which starts with the pre-measurements and progresses through non-unitary and ill-understood stages need not happen quite as fast in order to prevent the unstable state from decaying.

To complete our understanding of the quantum Zeno and anti-Zeno effects, a better understanding of the entire sequence of events that is involved in the act of measuring a quantum system is needed. Using our model we can pose the question whether the act of measurement can indeed be split into a pre-measurement part where there is a direct interaction between the system that is being observed and some part of the detector, entangling the two and a second part where this entanglement is transformed into a classically observable signal. The model suggests that the final outcomes of the measurement depends on the specific way the pre-measurement occurs. One of the potentially observable consequences of the pre-measurement is that under suitable conditions the 'Zeno time' can be made much larger than what one would expect of the system when it is evolving without interacting with the detector.

Acknowledgments

The guidance, inspiration and enlightenment provided by Professor E C G Sudarshan while pursuing the investigations presented in this paper are gratefully acknowledged by the author. I thank Professor T F Jordan and Mr Kavan Modi for helpful discussions and remarks and the referees for providing valuable suggestions that helped me improve this paper significantly. This work is supported in part by the U S Navy—Office of Naval Research grant no. N00014-03-1-0639.

Appendix. Orthonormality of the eigenstates of H

For equation (29) to be valid we have to show that the eigenstates of H are orthonormal, i.e.

$$\begin{aligned}\left(\Psi_\mu^{(1,2)}, \Psi_\lambda^{(1,2)}\right) &= \eta_\mu^* \eta_\lambda + \int_0^\infty \mathrm{d}\omega' \phi_\mu^*(\omega')\phi_\lambda(\omega') + \int_0^\infty \mathrm{d}\omega' \int_0^\infty \mathrm{d}\nu' \psi_\mu^{(\omega')*}(\nu')\psi_\lambda^{(\omega')}(\nu') \\ &= \delta(\lambda - \mu) \end{aligned} \tag{A.1}$$

A.1. Orthonormality of the first set of eigenstates $\Psi_\Lambda^{(1)}$

We start from the last term of $\left(\Psi_\mu^{(1)}, \Psi_\lambda^{(1)}\right)$,

$$\begin{aligned} I_3 &= \int_0^\infty \mathrm{d}\omega' \int_0^\infty \mathrm{d}\nu' \psi_\mu^{(\omega')*}(\nu')\psi_\lambda^{(\omega')}(\nu') \\ &= \int_0^\infty \mathrm{d}\omega' \int_0^\infty \mathrm{d}\nu' \left[e\delta(\mu - m_B - \nu')\delta(\omega' - \nu') + \frac{G^*(\omega', \nu')\phi_\mu^*(\omega')}{\mu - m_B - \nu' - \mathrm{i}\epsilon} \right] \end{aligned}$$

$$\times\left[e\delta(\lambda-m_B-\nu')\delta(\omega'-\nu')+\frac{G(\omega',\nu')\phi_\lambda(\omega')}{\lambda-m_B-\nu'+\mathrm{i}\epsilon}\right]$$
$$=\mathrm{e}^2\delta(\lambda-\mu)+\frac{eG(\mu-m_B,\mu-m_B)}{\lambda-\mu+\mathrm{i}\epsilon}\phi_\lambda(\mu-m_B)$$
$$-\frac{eG^*(\lambda-m_B,\lambda-m_B)}{\lambda-\mu-\mathrm{i}\epsilon}\phi^*_\mu(\lambda-m_B)+\int_0^\infty \mathrm{d}\omega'\frac{\phi^*_\mu(\omega')\phi_\lambda(\omega')}{\lambda-\mu+2\mathrm{i}\epsilon}$$
$$\times\left[\int_0^\infty \mathrm{d}\nu'\left(\frac{|G(\omega',\nu')|^2}{\mu-m_B-\nu'-\mathrm{i}\epsilon}-\frac{|G(\omega',\nu')|^2}{\lambda-m_B-\nu'+\mathrm{i}\epsilon}\right)\right]. \tag{A.2}$$

The last term in (A.2) can be simplified using

$$\int_0^\infty \mathrm{d}\omega'\frac{|G(\omega',\nu')|^2}{\lambda-m_B-\nu'+\mathrm{i}\epsilon}=\lambda-m_B-\omega'-\beta(\lambda,\omega')$$

to read

$$-\int_0^\infty \mathrm{d}\omega'\phi^*_\mu(\omega')\phi_\lambda(\omega')+\frac{1}{\lambda-\mu+2\mathrm{i}\epsilon}\int_0^\infty \mathrm{d}\omega'[\beta(\lambda,\omega')-\beta^*(\mu,\omega')]\phi^*_\mu(\omega')\phi_\lambda(\omega'). \tag{A.3}$$

The first term in the above expression cancels the second term in (A.1) and we obtain

$$\left(\Psi^{(1)}_\mu,\Psi^{(1)}_\lambda\right)=e^2\delta(\lambda-\mu)+\eta^*_\mu\eta_\lambda+\frac{eG(\mu-m_B,\mu-m_B)}{\lambda-\mu+\mathrm{i}\epsilon}\left[\frac{f(\mu-m_B)}{\beta(\lambda,\mu-m_B)}\eta_\lambda\right.$$
$$\left.+\frac{eG^*(\mu-m_B,\lambda-m_B)}{\beta(\lambda,\mu-m_B)}\delta(\lambda-\mu)\right]-\frac{eG^*(\lambda-m_B,\lambda-m_B)}{\lambda-\mu-\mathrm{i}\epsilon}$$
$$\times\left[\frac{f^*(\lambda-m_B)}{\beta^*(\mu,\lambda-m_B)}\eta^*_\mu+\frac{eG(\lambda-m_B,\mu-m_B)}{\beta^*(\mu,\lambda-m_B)}\delta(\lambda-\mu)\right]$$
$$+\frac{1}{\lambda-\mu+2\mathrm{i}\epsilon}\int_0^\infty \mathrm{d}\omega'[\beta(\lambda,\omega')-\beta^*(\mu,\omega')]\phi^*_\mu(\omega')\phi_\lambda(\omega'). \tag{A.4}$$

The two terms with $\delta(\lambda-\mu)$ in the above expression cancel each other thereby simplifying the expression to

$$\left(\Psi^{(1)}_\mu,\Psi^{(1)}_\lambda\right)=e^2\delta(\lambda-\mu)+\eta^*_\mu\eta_\lambda-\frac{e}{\lambda-\mu+\mathrm{i}\epsilon}\left[\frac{G^*(\lambda-m_B,\lambda-m_B)f^*(\lambda-m_B)}{\beta^*(\mu,\lambda-m_B)}\eta^*_\mu\right.$$
$$\left.-\frac{G(\mu-m_B,\mu-m_B)f(\mu-m_B)}{\beta(\lambda,\mu-m_B)}\eta_\lambda\right]$$
$$+\frac{1}{\lambda-\mu+2\mathrm{i}\epsilon}\int_0^\infty \mathrm{d}\omega'[\beta(\lambda,\omega')-\beta^*(\mu,\omega')]\phi^*_\mu(\omega')\phi_\lambda(\omega'). \tag{A.5}$$

The last term in (A.5) can be expanded as follows:

$$\frac{1}{\lambda-\mu+2\mathrm{i}\epsilon}\int \mathrm{d}\omega'[\beta(\lambda,\omega')-\beta^*(\mu,\omega')]\left[\frac{f(\omega')}{\beta(\lambda,\omega')}\eta_\lambda+\frac{eG^*(\omega',\lambda-m_B)}{\beta(\lambda,\omega')}\delta(\lambda-m_B-\omega')\right]$$
$$\times\left[\frac{f^*(\omega')}{\beta^*(\mu,\omega')}\eta^*_\mu+\frac{eG(\omega',\mu-m_B)}{\beta^*(\mu,\omega')}\delta(\mu-m_B-\omega')\right]$$

$$=\frac{\eta^*_\mu\eta_\lambda}{\lambda-\mu+2\mathrm{i}\epsilon}\int_0^\infty \mathrm{d}\omega'\left[\frac{|f(\omega')|^2}{\beta^*(\mu,\omega')}-\frac{|f(\omega')|^2}{\beta(\lambda,\omega')}\right]+\frac{\alpha^*(\mu)-\alpha(\lambda)}{\lambda-\mu+2i\epsilon}\eta^*_\mu\eta_\lambda$$
$$+\frac{e}{\lambda-\mu+2\mathrm{i}\epsilon}\left[\frac{G^*(\lambda-m_B,\lambda-m_B)f^*(\lambda-m_B)}{\beta^*(\mu,\lambda-m_B)}\eta^*_\mu\right.$$

$$- \frac{G(\mu - m_B, \mu - m_B) f(\mu - m_B)}{\beta(\lambda, \mu - m_B)} \eta_\lambda \Bigg]$$
$$+ \frac{e^2 \delta(\lambda - \mu)}{\lambda - \mu + 2\mathrm{i}\epsilon} \Bigg[\frac{G^*(\lambda - m_B, \lambda - m_B) f^*(\lambda - m_B)}{\beta^*(\mu, \lambda - m_B)}$$
$$- \frac{G(\mu - m_B, \mu - m_B) f(\mu - m_B)}{\beta(\lambda, \mu - m_B)} \Bigg] \tag{A.6}$$

where we have used

$$\alpha(\lambda)\eta_\lambda = \frac{G^*(\lambda - m_B, \lambda - m_B) f^*(\lambda - m_B)}{\beta^*(\mu, \lambda - m_B)},$$
$$\alpha^*(\mu)\eta_\mu^* = \frac{G(\mu - m_B, \mu - m_B) f(\mu - m_B)}{\beta(\lambda, \mu - m_B)}.$$

The last term in (A.6) is zero while

$$\frac{\eta_\mu^* \eta_\lambda}{\lambda - \mu + 2\mathrm{i}\epsilon} \int_0^\infty \mathrm{d}\omega' \left[\frac{|f(\omega')|^2}{\beta^*(\mu, \omega')} - \frac{|f(\omega')|^2}{\beta(\lambda, \omega')} \right] = -\eta_\mu^* \eta_\lambda - \frac{\alpha^*(\mu) - \alpha(\lambda)}{\lambda - \mu + 2\mathrm{i}\epsilon} \eta_\mu^* \eta_\lambda$$

using

$$\int_0^\infty \mathrm{d}\omega' \frac{|f(\omega')|^2}{\beta^*(\mu, \omega')} = \mu - m_A - \alpha^*(\mu); \qquad \int_0^\infty \mathrm{d}\omega' \frac{|f(\omega')|^2}{\beta(\lambda, \omega')} = \lambda - m_A - \alpha(\lambda).$$

So putting all the terms together we obtain

$$\left(\Psi_\mu^{(1)}, \Psi_\lambda^{(1)}\right) = e^2 \delta(\lambda - \mu)$$

which also implies that $e = \pm 1$ (we choose $e = +1$).

A.2. Orthonormality of the second set of eigenstates $\Psi_\Lambda^{(2)}$

The last term of $\left(\Psi_\mu^{(2)}, \Psi_\lambda^{(2)}\right)$ is

$$I_3 = \int_0^\infty \mathrm{d}\omega' \int_0^\infty \mathrm{d}\nu' \psi_\mu^{(\omega')*}(\nu') \psi_\lambda^{(\omega')}(\nu')$$
$$= \int_0^\infty \mathrm{d}\omega' \frac{\phi_\mu^*(\omega')\phi_\lambda(\omega')}{\lambda - \mu + 2\mathrm{i}\epsilon} \left[\int_0^\infty \mathrm{d}\nu' \left(\frac{|G(\omega', \nu')|^2}{\mu - m_B - \nu' - \mathrm{i}\epsilon} - \frac{|G(\omega', \nu')|^2}{\lambda - m_B - \nu' + \mathrm{i}\epsilon} \right) \right]$$
$$= -\int_0^\infty \mathrm{d}\omega' \phi_\mu^*(\omega')\phi_\lambda(\omega') + \frac{1}{\lambda - \mu + 2\mathrm{i}\epsilon} \int_0^\infty \mathrm{d}\omega' [\beta(\lambda, \omega') - \beta^*(\mu, \omega')] \phi_\mu^*(\omega')\phi_\lambda(\omega')$$

using equation (A.3). We now obtain

$$\left(\Psi_\mu^{(2)}, \Psi_\lambda^{(2)}\right) = \eta_\mu^* \eta_\lambda + \frac{1}{\lambda - \mu + 2\mathrm{i}\epsilon} \int_0^\infty \mathrm{d}\omega' [\beta(\lambda, \omega') - \beta^*(\mu, \omega')] \phi_\mu^*(\omega')\phi_\lambda(\omega'). \tag{A.7}$$

The explicit solution of the model in equation (23) can be used to write the second term in the above expression as

$$\frac{1}{\lambda - \mu + 2\mathrm{i}\epsilon} \int_0^\infty \mathrm{d}\omega' [\beta(\lambda, \omega') - \beta^*(\mu, \omega')] \left[\frac{f(\omega')}{\beta(\Lambda, \omega')} \eta_\Lambda + \tilde{e}_\Lambda \delta(\Lambda - m_B - \mathcal{K}_\Lambda - \omega') \right]$$
$$\times \left[\frac{f^*(\omega')}{\beta^*(\mu, \omega')} \eta_\mu^* + \tilde{e}_\mu \delta(\mu - m_B - \mathcal{K}_\mu - \omega') \right]$$
$$= \tilde{e}^2 \frac{\beta(\lambda, \mu - m_B - \mathcal{K}_\mu) - \beta^*(\mu, \mu - m_B - \mathcal{K}_\mu)}{\lambda - \mu + 2\mathrm{i}\epsilon} \delta(\lambda - \mu)$$
$$+ \frac{\eta_\mu^* \eta_\lambda}{\lambda - \mu + 2\mathrm{i}\epsilon} \int_0^\infty \mathrm{d}\omega' \left[\frac{|f(\omega')|^2}{\beta^*(\mu, \omega')} - \frac{|f(\omega')|^2}{\beta(\lambda, \omega')} \right] + \frac{\alpha^*(\mu) - \alpha(\lambda)}{\lambda - \mu + 2i\epsilon} \eta_\mu^* \eta_\lambda.$$

The last two terms in the above expression can be reduced to $-\eta_\mu^*\eta_\lambda$, which cancels the first term in (A.7) and we are left with

$$\left(\Psi_\mu^{(2)}, \Psi_\lambda^{(2)}\right) = \tilde{e}^2\delta(\lambda-\mu)\beta'_\lambda$$

where

$$\begin{aligned}\beta'_\lambda &= \frac{\mathrm{d}}{\mathrm{d}\lambda}\beta(\lambda,\omega)\bigg|_{\omega=\lambda-m_B-\mathcal{K}_\lambda} \\ &= \lim_{\epsilon\to 0}\lim_{\lambda\to\mu}\frac{\beta(\lambda+\mathrm{i}\epsilon, \lambda-m_B-\mathcal{K}_\lambda)-\beta(\mu-\mathrm{i}\epsilon,\mu-m_B-\mathcal{K}_\mu)}{\lambda-\mu+2\mathrm{i}\epsilon}. \end{aligned} \tag{A.8}$$

We have used $\beta^*(\lambda+\mathrm{i}\epsilon,\omega)=\beta(\lambda-\mathrm{i}\epsilon,\omega)$ in the above expression. For orthonormality we see that $\tilde{e}=(\beta'_\lambda)^{-1/2}$.

We leave it to the reader to verify that $\left(\Psi_\lambda^{(1)}, \Psi_\mu^{(2)}\right)=0$, completing the demonstration of the orthonormality of the eigenstates of the Hamiltonian of our model. The same techniques used here can be employed to show the completeness of the eigenstates of H that we obtained. Since this is a lengthy and detailed calculation that closely follows the proof of completeness of the eigenstates of the Cascade model, we refer the reader to the extensive discussion in [6] to see how to proceed with the calculation.

References

[1] Misra B and Sudarshan E C G 1977 *J. Math. Phys.* **18** 756
[2] Wheeler J A and Zurek W H 1983 *Quantum Thoery and Measurement* (Princeton, NJ: Princeton University Press)
[3] Zurek W H 2003 *Rev. Mod. Phys.* **75** 715
[4] Sudarshan E C G 1976 *Pramana J. Phys.* **6** 117
[5] Sherry T N and Sudarshan E C G 1978 *Phys. Rev.* D **18** 4580
[6] Chiu C B, Sudarshan E C G and Bhamathi G 1992 *Phys. Rev.* D **46** 3508
[7] Kaulakys B and Gontis V *Phys. Rev.* A **56** 1131
[8] Lewenstein M and Rzazewski K 2000 *Phys. Rev.* A **61** 022105
[9] Kofman A G and Kurizki G 2000 *Nature* **405** 546
[10] Facchi P, Nakazato H and Pascazio S 2001 *Phys. Rev. Lett.* **86** 2699
[11] Neumann J-v 1955 *Mathematical Foundations of Quantum Mechanics* (Princeton, NJ: Princeton University Press)
[12] Atmanspacher H, Ehm W and Gneiting T 2003 *J. Phys. A: Math. Gen.* **36** 9899
[13] Exner P and Ichinose T 2003 *Preprint* math-ph/0302060
[14] Schmidt A U 2002 *J. Phys. A: Math. Gen.* **35** 7817
[15] Schmidt A U 2003 *J. Phys. A: Math. Gen.* **36** 1135
[16] Ruseckas J and Kaulakys B 2001 *Phys. Rev.* A **63** 062103
[17] Ruseckas J 2001 *Phys. Lett.* A **291** 185
[18] Peres A 1993 *Quantum Theory: Concepts and Methods* (Dordrecht: Kluwer)
[19] Fearn H J and Lamb W E 1992 *Phys. Rev.* A **46** 1199
[20] Altenmuller T P and Schenzle A 1994 *Phys. Rev.* A **49** 2016
[21] Wallace D 2001 *Phys. Rev.* A **63** 022109
[22] Itano W M, Heinzen D J, Bollinger J J and Wineland D J 1990 *Phys. Rev.* A **41** 2295
[23] Wunderlich C, Balzer C and Toschek P E 2001 *Z. Naturforsch* **56** 160
[24] Fischer M C, Gutierrez-Medina B and Raizen M G 2001 *Phys. Rev. Lett.* **87** 040402
[25] Valanju P 1980 *PhD Thesis* University of Texas at Austin
[26] Modi K A and Shaji A, Quantum Zeno and anti-zeno effects in an unstable two dsicrete level system coupled to a continuum (unpublished)
[27] Wigner E P 1963 *Am. J. Phys.* **31** 6
[28] Peres A 1980 *Phys. Rev.* D **22** 879
[29] Chiu C B, Sudarshan E C G and Misra B 1977 *Phys. Rev.* D **16** 520
[30] Valanju P, Sudarshan E C G and Chiu C B 1980 *Phys. Rev.* D **21** 1304
[31] Petrosky T, Tasaki S and Prigogine I 1990 *Phys. Lett.* A **151** 109

[32] Petrosky T, Tasaki S and Prigogine I 1991 *Physica* A **170** 306
[33] Sudarshan E C G, Chiu C B and Bhamathi G 1997 *Unstable Systems in Generalized Quantum Theory (Advances in Chemical Physics XCIX)* (New York: Wiley) p 121–210
[34] Antoniou I, Karpov E, Pronko G and Yarevsky E 2001 *Phys. Rev.* A **63** 062110
[35] Breit G and Wigner E P 1936 *Phys. Rev.* **49** 519
[36] Dirac P A M 1970 *The Principles of Quantum Mechanics* 4th edn (Oxford: Clarendon)
[37] Khalfin L A 1958 *Sov. Phys.—JETP* **6** 1503
[38] Wilkinson S R, Bharucha C F, Fischer M C, Madison K W, Morrow P R, Niu Q, Sundaram B and Raizen M G 1997 *Nature* **387** 575
[39] Nakazato H, Namiki M and Pascazio S 1996 *Int. J. Mod. Phys.* B **10** 247
[40] Koshino K and Shimizu A 2003 *Phys. Rev.* A **67** 42101
[41] Koshino K and Shimizu A 2004 *Phys. Rev. Lett.* **92** 030401
[42] Schulman L S 1998 *Phys. Rev.* A **57** 1509
[43] Panov A D 2000 *Physica* A **287** 193
[44] Facchi P and Pascazio S 2000 *Phys. Rev.* A **62** 023804
[45] Schweber S S 1962 *An Introduction to Relativistic Quantum Field Theory* (New York: Harper and Row)
[46] Lee T D 1954 *Phys. Rev.* **95** 1329
[47] Friedrichs K O 1948 *Commun. Pure Appl. Math.* **1** 361
[48] Sudarshan E C G 1962 *Relativistic Particle Interactions in Proc Brandeis Summer Institute on Theoretical Physics* (New York: Benjamin)